A High-Efficiency Diplexer for Sustainable 5G-Enabled IoT in Metaverse Transportation System and Smart Grids

Mohammad (Behdad) Jamshidi [1], Salah I. Yahya [2,3], Leila Nouri [4,5,*], Hamed Hashemi-Dezaki [6,*], Abbas Rezaei [7] and Muhammad Akmal Chaudhary [8]

1 Faculty of Electrical Engineering, University of West Bohemia, Univerzitní 22, 306 14 Pilsen, Czech Republic
2 Department of Communication and Computer Engineering, Cihan University-Erbil, Erbil 44001, Iraq
3 Department of Software Engineering, Faculty of Engineering, Koya University, Koya KOY45, Iraq
4 Institute of Research and Development, Duy Tan University, Da Nang 550000, Vietnam
5 School of Engineering & Technology, Duy Tan University, Da Nang 550000, Vietnam
6 Research and Innovation Center for Electrical Engineering (RICE), Faculty of Electrical Engineering, University of West Bohemia (UWB), 301 00 Pilsen, Czech Republic
7 Department of Electrical Engineering, Kermanshah University of Technology, Kermanshah 6715685420, Iran
8 Department of Electrical and Computer Engineering, Ajman University, Ajman 00000, United Arab Emirates
* Correspondence: leilanouri@duytan.edu.vn (L.N.); hhashemi@fel.zcu.cz (H.H.-D.)

Abstract: Symmetry is essential in the design of complex systems like the Metaverse Transportation Sys-tem (MTS) and helps ensure that all components work together effectively. In the development of a microstrip diplexer for 5G-enabled IoT and MTS, maintaining symmetry is crucial to achieving flat responses with low group delays. By integrating transportation technology and the Metaverse, the Metaverse Transportation System (MTS) can greatly improve the effectiveness and intellect of transportation systems in reality. To establish a dependable network, it is essential to include 5G-enabled Internet of Things (IoT) and sensor networks with a sustainable design that focuses on efficiency and energy conservation. A three-channel microstrip lowpass-bandpass diplexer has been developed for 5G-enabled IoT and MTS implementation. Multi-channel designs are rare due to the complex design process, but this diplexer is very compact at only 0.004 $\lambda_g{}^2$. All channels have flat responses with group delays of 0.34 ns, 1.7 ns, and 0.34 ns at the lower, middle, and upper passbands, respectively. The lowpass channel has a cut-off frequency of 1.22 GHz, suitable for mid-band 5G applications. Compared to previous work, this diplexer achieves the smallest size, lowest group delay, and insertion and return losses at the lower channel. It consists of a lowpass-bandpass section connected to a band-pass filter analyzed mathematically, and its performance has been verified through simulation and measurement with good accuracy.

Keywords: sustainability; metaverse; diplexer; 5G; smart grids; diplexer; IoT; intelligent transportation systems

1. Introduction

In recent times, the concept of Big Data has gained immense popularity in both academic and industrial domains. It refers to massive and intricate data sets that are obtained from various sources. Many of the most well-known data processing techniques involve the use of Big Data techniques such as social networks, data fusion, artificial intelligence, machine learning, data mining, and others. Numerous individuals across various fields use Big Data analytics and have achieved significant accomplishments. For instance, in the business sector, some enterprises utilize Big Data to gain a better understanding of consumer behavior, optimize product pricing, enhance operational efficiency, and reduce staffing costs [1]. In addition, those with foresight anticipate that autonomous vehicles will surpass human drivers, resulting in smoother traffic flow, reduced delays, less pollution,

and improved comfort for both drivers and passengers. Nevertheless, the intricate management of a large number of vehicles through distributed control is a significant challenge that cannot be underestimated. For instance, in the event of a natural disaster such as an earthquake, it is essential for autonomous vehicles to quickly and efficiently coordinate the evacuation of critical areas [2].

On the other hand, the virtual transportation space consists of several elements such as static objects, dynamic objects, seasons, weather, and light sources. The appearance properties of static objects in virtual space resemble those of the physical space, whereas dynamic objects should have functional properties similar to real targets. The weather and season directly affect the rendering effect, which should adhere to physical laws, for instance, plants blooming in spring and sunlight during the day, and the use of streetlights and car lights at night. Ensuring the accuracy of the virtual space can significantly decrease the gap between the two parallel spaces [3]. The Metaverse, which is a term used to describe a virtual world that exists alongside the physical world, can play a crucial role in this area. While it was initially a theoretical concept, it has now become a reality in virtual reality games [4]. The Metaverse has potential applications in various industries, such as marketing, education, social media, and advertising. However, there has been minimal exploration of its potential uses in the transportation sector [5].

As the Metaverse becomes more prevalent, it opens up new possibilities for bridging the gap between the physical and virtual transportation spaces. Virtual transportation models can benefit from the realistic rendering of static and dynamic objects, weather, and light sources. In particular, the design of microstrip multi-band diplexers can play a crucial role in modern multi-channel communication systems for transportation. However, due to the complexity of the design process, microstrip lowpass-bandpass diplexers have been less explored, and multi-band diplexers are less commonly designed than dual-band ones. In this context, the development of efficient and compact three-band microstrip diplexers can address the limitations of existing devices and open new opportunities for the transportation sector.

Microstrip multi-band diplexers play an important role in modern multi-channel communication systems to separate the desired signals and pass them from two ports [6,7]. Due to the complexity of the design process, microstrip lowpass-bandpass diplexers have been less reported [8,9]. Moreover, multi-band diplexers are less designed than dual-band ones [10,11]. Dual-/three-band bandpass filters (BPFs) and diplexer have been reported in [12]. Microstrip triplexers are a type of multiplexer with three-channels that are suitable for multi-channel communication systems [13–15]. Generally, the common disadvantages of these devices [6–9,11–15] are high insertion losses (ILs), except from [10], and limited bandwidths. Due to the convenient design process, a high number of the dual-channel bandpass-bandpass diplexers have been reported [16,17]. In this type of diplexers, usually only a BPF was designed; then, it was copied with a larger (or smaller) scale. The overall sizes of the proposed microstrip devices in [6–9,11–18] are large. However, three-band diplexers are rarely designed.

In this work, we design a microstrip lowpass-bandpass diplexer with three separate passbands. Our goal is to miniaturize and achieve a good frequency response. The presented diplexer includes a lowpass-bandpass cell and a BPF. The insertion losses at all channels are low. The design process is summarized as follows: First, a lowpass-bandpass resonator is proposed and its equivalent *LC* circuit is analyzed. Then, a BPF is designed and analyzed. Both BPF and lowpass-bandpass resonator are optimized to achieve a high performance. Finally, the BPF and lowpass-bandpass resonator are integrated to obtain our three-channel lowpass-bandpass diplexer. A comparison between the proposed fabricated structure and the other reported diplexers and triplexers are presented in terms of size and efficiency. The comparison results show that we could reduce the IL drastically with the smallest size, while the fractional bandwidth (FBW) of our diplexer is wide.

The efficient energy consumption and operation of telecommunication infrastructures for IoT is a major challenge due to the requirement of supporting numerous low-power de-

vices with limited battery life. To address this challenge, the development of energy-efficient communication protocols and network architectures that minimize energy consumption in both devices and the underlying infrastructure is necessary. Microstrip components offer a solution to improve energy consumption and efficiency in IoT and telecommunication infrastructures through their ability to provide cost-effective, low-loss, and compact solutions. Microstrip filters, diplexers, and antennas can be designed to operate at desired frequencies with high selectivity, low insertion loss, and high-power handling capability, thereby helping to alleviate the energy consumption challenge in the telecommunication infrastructure for IoT.

The work presented several important contributions, including the conceptualization of an integrated framework based on the Metaverse Transportation System, smart grid, and 5G-enabled IoT; demonstrating the role of 5G-enabled IoTs; designing and fabricating a high-efficiency diplexer for 5G-enabled IoT; and developing a diplexer with impressive qualities in terms of size and performance.

(1) High-Efficiency Diplexer for 5G-Enabled IoT has been designed, fabricated, and measured based on the requirement for the framework: The researchers have designed, fabricated, and tested a component called a diplexer, which is an essential infrastructure for 5G-enabled IoTs. This diplexer is highly efficient and was created based on the requirements of the integrated framework.

(2) The role of 5G-enabled IoTs has been demonstrated: The researchers have shown the importance of 5G-enabled Internet of Things in creating a dependable network for the integrated framework. They have emphasized the need for sustainable design that focuses on efficiency and energy conservation.

(3) An integrated framework based on the Metaverse Transportation System, smart grid, and 5G-enabled IoT has been conceptualized: This means that the researchers have come up with a theoretical framework that combines the Metaverse Transportation System, smart grid technology, and 5G-enabled Internet of Things. This framework has the potential to significantly enhance the efficiency and intelligence of transportation systems in reality.

(4) The proposed Diplexer has some astonishing features in terms of size and performance, making it a brilliant candidate for the 5G-enabled IoTs: The diplexer that was designed and fabricated has some impressive qualities in terms of size and performance.

This paper presents the design process of a super-efficient diplexer and its application in a framework that includes the integration of the MTS and smart grids for 5G-enabled IoT. The organization of the paper is as follows: Section 2 introduces the MTS, which utilizes virtual reality technology to provide an immersive transportation experience, and the diplexer technology, which is a significant component in 5G-enabled IoT. Section 3 provides a detailed analysis of the proposed three-band diplexer, including its performance in terms of insertion loss, return loss, and isolation. Section 4 presents simulation and measurement results to validate the accuracy and real-world performance of the diplexer. Section 5 discusses the potential applications of this technology and its impact on the future of transportation and communication. In conclusion, this paper proposes a new technology that has the potential to revolutionize transportation, leading to new opportunities for innovation and growth.

2. Metaverse Transportation System and Diplexer for 5G-Enabled IoT

Intelligent Transportation Systems (ITS) utilize sensor equipment to collect various types of information, such as vehicle speeds, traffic flows, trip times, and vehicle density. Wide area data pertaining to the comprehensive traffic flow data are gathered using various sensor tracking techniques such as space-based radar, video processing, photogrammetric processing, and sound recording [1]. Moreover, virtualization is a crucial aspect of cloud computing and is especially important in the context of Vehicular Cloud Computing (VCC) and supporting autonomous vehicles (AUVs). AUVs are equipped with numerous sensors and may need to perform tasks such as recognizing individuals in a certain geographic area.

The AUVs can filter and correlate initial data, but the final processing must be uploaded to a virtual image of the pattern recognition process in the Internet cloud. Virtualization is also necessary to protect driver privacy and ensure application sensitivity. In addition to offloading complex computations to the cloud [19], virtualization can customize the sensor platform for different applications. For instance, a car manufacturer may access all Controller Area Network (CAN) bus sensors and cameras, while a neighbor vehicle may only access outward-facing cameras [2].

Intelligent Transportation System (ITS) and the Metaverse are innovative technologies that have the power to revolutionize the current transportation system by reducing traffic accidents and enhancing driving safety. By merging transportation technology and the Metaverse into a single Metaverse Transportation System (MTS), there is a tremendous potential to augment the intelligence of real-world transportation systems.

The advanced digital models created in the MTS enable a complete simulation of the lifecycle of physical objects, thereby empowering the virtual space with greater control and adaptability. Consequently, the integration of Metaverse and transportation technology through the MTS has the ability to bring about a significant transformation in the transportation industry by enhancing its efficiency, safety, and intelligence [3].

Regarding energy management, incorporating 5G-enabled Internet of Things (IoT) technology into edge computing smart grids and the Metaverse can significantly improve its effectiveness. By utilizing sensors and meters, smart grids can collect real-time data on energy consumption and generation from various nodes, which can then be analyzed to optimize energy distribution and utilization [20,21]. Additionally, IoT infrastructure allows for remote control of energy consumption and generation devices, enabling more efficient energy usage. Moreover, the Metaverse, an immersive virtual world, can also contribute to energy management by offering users an interactive platform to monitor and manage their energy consumption [22].

With the use of smart devices and IoT infrastructure, users can control their energy usage within the Metaverse, creating an immersive experience while simultaneously reducing their energy costs. Integrating IoT technology in smart grids and the Metaverse can also benefit energy providers, as they can use the real-time data collected using IoT sensors to improve their energy production and distribution processes. This can lead to more efficient use of resources, reduced energy waste, and lower costs for both providers and end-users.

Figure 1 illustrates the proposed framework for 5G enabled IoT in the MTS. The Metaverse Transportation System and Smart Grids framework is designed to enhance the quality of intelligent transportation systems, taking into account the advancements in technology such as the Metaverse, 5G enabled IoT, and smart grids. This framework comprises five layers, each serving a specific purpose in optimizing the transportation system.

The first layer of the framework is the Metaverse Transportation System. This layer allows users to experience the benefits of the Metaverse in an immersive environment. The Metaverse is a virtual world that enables individuals to interact with each other and the environment seamlessly and naturally. The Metaverse Transportation System leverages this technology to provide a more intuitive and personalized experience for transportation users. The second layer of the framework is Smart Grids for Intelligent Transportation Systems. Smart grids are modern electricity grids that use advanced technologies such as sensors, communications, and analytics to optimize the generation, distribution, and consumption of energy.
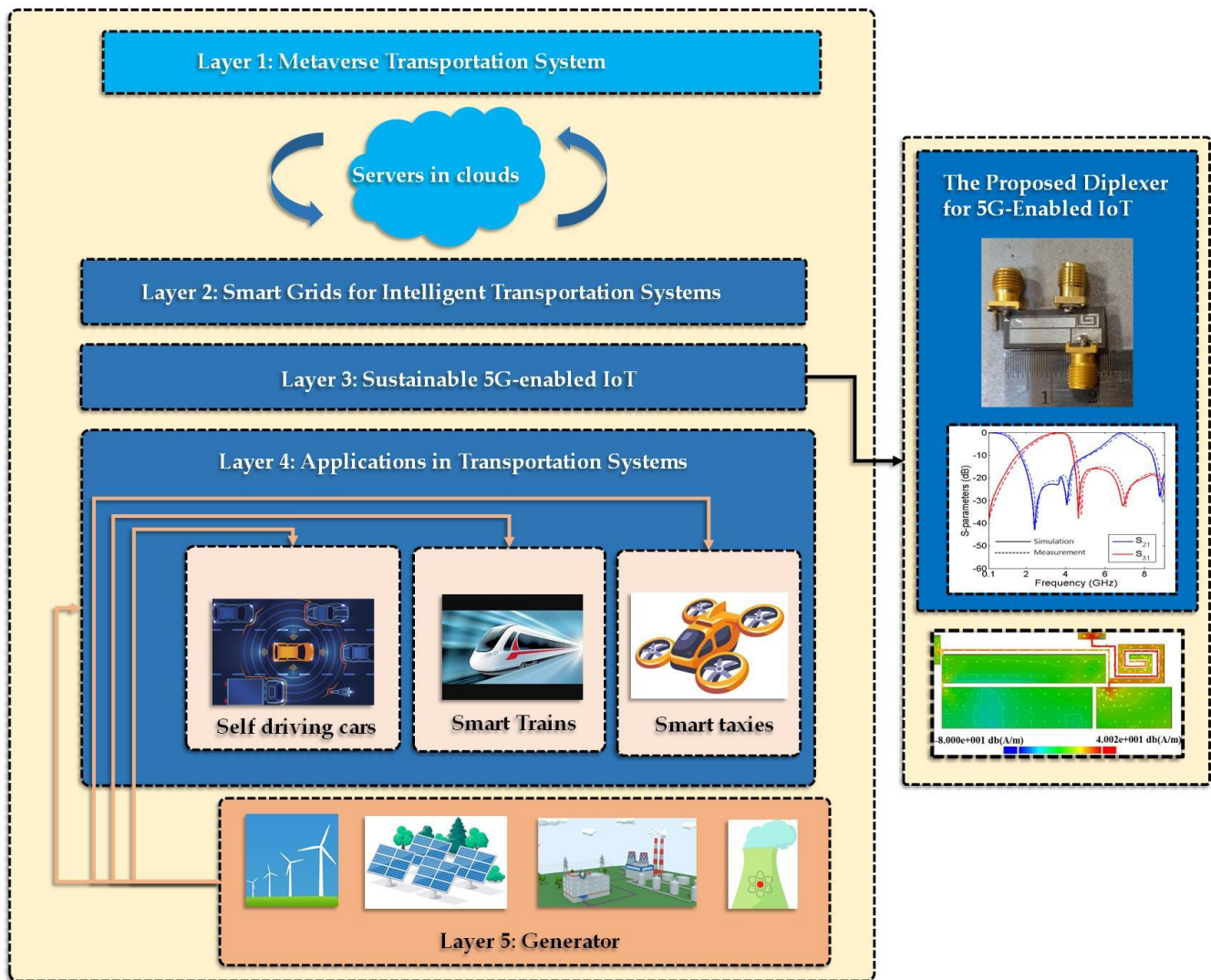
Figure 1. The proposed framework for the MTS and smart grids. This framework consists of five layers designed to enhance the quality of intelligent transportation systems. Layer 1 is the Metaverse Transportation System, layer 2 is Smart Grids for Intelligent Transportation Systems, layer 3 is Sustainable 5G-enabled IoT, layer 4 is Applications in Transportation Systems, and layer 5 is Generators and Power Plants. The framework leverages advanced technologies such as the Metaverse, smart grids, and 5G-enabled IoT, and autonomous vehicles to provide a seamless and efficient transportation experience. Each layer serves a specific purpose in optimizing the transportation system, resulting in a comprehensive approach to transportation system management.

In the context of intelligent transportation systems, smart grids can help ensure that the power supply for electric vehicles is stable and reliable. The third layer of the framework is Sustainable 5G-enabled IoT. This layer involves the use of 5G-enabled IoT devices, which are connected to the internet and can communicate with other devices. These devices are designed to be energy-efficient, with low power requirements and longer battery life. Our proposed diplexer serves as an important communication component in this layer, enabling the transfer of data between different devices. The fourth layer of the framework is Applications in Transportation Systems. This layer covers autonomous vehicles, smart trains, and smart taxis. These applications rely on advanced technologies such as sensors, cameras, and machine learning algorithms to optimize their operations. The Metaverse Transportation System and Smart Grids framework can provide these applications with the necessary infrastructure and support to operate efficiently and effectively. Finally,

the fifth layer of the framework is Generators and Power Plants. This layer focuses on how generators can be controlled by the Metaverse Transportation System. By integrating generators into the framework, we can ensure that the power supply for transportation systems is stable and reliable, even during peak usage periods. In conclusion, the Metaverse Transportation System and Smart Grids framework is a comprehensive approach to optimizing transportation systems. It leverages advanced technologies such as the Metaverse, smart grids, 5G-enabled IoT, and autonomous vehicles to provide a seamless and efficient transportation experience. The transportation system's success is ensured by a framework consisting of five layers, with each layer serving a specific purpose.

3. Analysis of the Proposed Three-Band Diplexer

Our predetermined goal is to design a three-band diplexer. We prefer to connect a lowpass-bandpass resonator to another bandpass resonator to create three passbands. The lowpass-bandpass resonator should have a lowpass and a bandpass channel. Figure 2 depicts the layout and an approximate equivalent LC circuit of this resonator. As shown in Figure 2, this resonator has two stubs 1 and 2, while the equivalents of them are C_1 and C_2, respectively. The equivalents of physical lengths l_a and l_b are presented by L_a and L_b, respectively. Since the effect of bents and steps are negligible at frequencies below 10 GHz, we have ignored them in the approximated LC circuit.
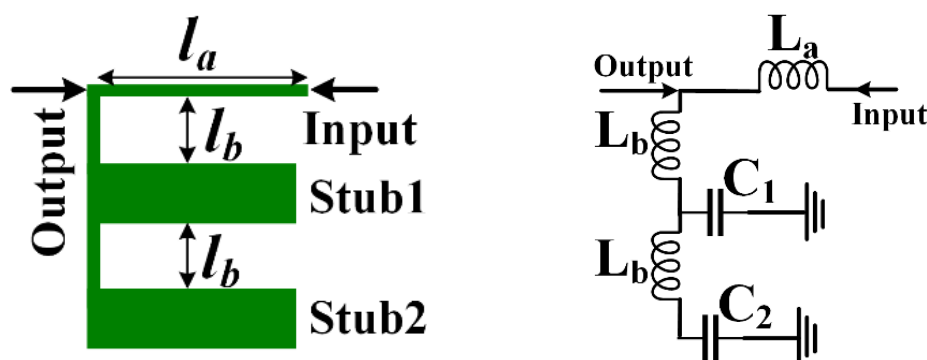

Figure 2. Lowpass-bandpass resonator and its approximate *LC* circuit.

To analyze this resonator, first, we calculate its transfer matrix (T) as follows:

$$T = \begin{bmatrix} A & B \\ C & D \end{bmatrix} = \begin{bmatrix} 1 & 0 \\ \frac{1}{Z_b} & 1 \end{bmatrix} \times \begin{bmatrix} 1 & j\omega L_a \\ 0 & 1 \end{bmatrix} = \begin{bmatrix} 1 & j\omega L_a \\ \frac{1}{Z_b} & 1 + \frac{j\omega L_a}{Z_b} \end{bmatrix}$$

$$Z_b = \frac{(\frac{1}{j\omega C_2} + j\omega L_b) \times \frac{1}{j\omega C_1}}{\frac{1}{j\omega C_2} + j\omega L_b + \frac{1}{j\omega C_1}} + j\omega L_b = (\frac{\omega^2 C_2 L_b - 1}{\omega C_2 (C_1 + 1) - \omega^3 C_2 C_1 L_b} + \omega L_b)j \tag{1}$$

where ω is an angular frequency. As shown in Equation (1), Z_b is the equivalent impedance from the output port to the grounded capacitor C_2. The transmission parameter S_{21} can be extracted from the transfer matrix as follows [23]:

$$S_{21} = \frac{2}{A + B/Z_0 + CZ_0 + D} \Rightarrow S_{21} = \frac{2}{2 + \frac{j\omega L_a}{Z_0} + \frac{Z_0}{Z_b} + \frac{j\omega L_a}{Z_b}} \tag{2}$$

where Z_0 is the impedance of terminals. The IL (insertion loss) will be calculated, from Equation (2), as follows:

$$IL = -20\log(|S_{21}|) \Rightarrow IL = -20\log\left(\left|\frac{2}{2 + \frac{j\omega L_a}{Z_0} + \frac{Z_0}{Z_b} + \frac{j\omega L_a}{Z_b}}\right|\right) \tag{3}$$

Since for having a passband, the IL should be a small value near zero, each condition for $|S_{21}| = 1$ leads to obtaining a passband. This condition will be obtained using the following equations:

$$IL = 0 \Leftrightarrow |S_{21}| = 1 \Rightarrow$$

$$\left| \frac{2}{2 + \frac{j\omega L_a}{Z_0} - Z_0 \left(\frac{\omega^2 C_2 L_b - 1}{\omega C_2 (C_1+1) - \omega^3 C_2 C_1 L_b} + \omega L_b \right)^{-1} j + \left(\frac{\omega^2 C_2 L_b - 1}{\omega C_2 (C_1+1) - \omega^3 C_2 C_1 L_b} + \omega L_b \right)^{-1} \omega L_a} \right| = 1 \Rightarrow$$

$$\begin{cases} \left(\frac{\omega^2 C_2 L_b - 1}{\omega C_2 (C_1+1) - \omega^3 C_2 C_1 L_b} + \omega L_b \right)^{-1} \omega L_a = 0 \Rightarrow \left(\frac{\omega^2 C_2 L_b - 1}{(\omega C_2 (C_1+1) - \omega^3 C_2 C_1 L_b)} + \omega L_b \right)^{-1} = 0 \Rightarrow \\[2mm] \omega C_2 (C_1 + 1) - \omega^3 C_2 C_1 L_b) = 0 \Rightarrow \begin{cases} \omega_1 = 0 \\ C_2(C_1+1) - \omega_2^2 C_2 C_1 L_b = 0 \rightarrow \omega_2 = \sqrt{\frac{C_1+1}{C_1 L_b}} \end{cases} \\[3mm] \frac{j\omega L_a}{Z_0} - Z_0 \left(\frac{\omega^2 C_2 L_b - 1}{\omega C_2 (C_1+1) - \omega^3 C_2 C_1 L_b} + \omega L_b \right)^{-1} j = 0 \Rightarrow \frac{\omega^2 L_b [C_2(C_1+2) - \omega^2 C_2 C_1 L_b] - 1}{C_2(C_1+1) - \omega^2 C_2 C_1 L_b} = \frac{Z_0^2}{L_a} \\[3mm] \Rightarrow \omega^4 C_2 C_1 L_b^2 L_a - \omega^2 L_b C_2 \left[C_1 Z_0^2 - L_a (C_1+2) \right] + L_a + C_2(C_1+1) Z_0^2 = 0 \\[3mm] \omega_3 = \sqrt{\frac{L_b C_2 \left[C_1 Z_0^2 - L_a (C_1+2) \right] - \sqrt{\left[L_b C_2 \left[C_1 Z_0^2 - L_a (C_1+2) \right] \right]^2 - 4 C_2 C_1 L_b^2 L_a \left(L_a + C_2(C_1+1) Z_0^2 \right)}}{2 C_2 C_1 L_b^2 L_a}} \\[5mm] \omega_4 = \sqrt{\frac{L_b C_2 \left[C_1 Z_0^2 - L_a (C_1+2) \right] + \sqrt{\left[L_b C_2 \left[C_1 Z_0^2 - L_a (C_1+2) \right] \right]^2 - 4 C_2 C_1 L_b^2 L_a \left(L_a + C_2(C_1+1) Z_0^2 \right)}}{2 C_2 C_1 L_b^2 L_a}} \end{cases} \tag{4}$$

where ω_1 and ω_2 are the main angular resonance frequencies and ω_3 and ω_4 are two harmonics that will be suppressed. A method to remove one harmonic will be obtained for $\omega_3 = 0$, which will be achieved for the very small value of $4 C_2 C_1 L_b^2 L_a (L_a + C_2(C_1+1) Z_0^2$ near zero. Another way to get rid of this harmonics and obtain $\omega_3 = 0$ is:

$$\left[L_b C_2 [C_1 Z_0^2 - L_a(C_1+2)] \right]^2 \rangle\rangle \, 4 C_2 C_1 L_b^2 L_a (L_a + C_2(C_1+1) Z_0^2) \tag{5}$$

Equation (5) is correct for the values of inductors and capacitors in nH and nF with a high precision. If the value of $L_b C_2 [C_1 Z_0^2 - L_a(C_1+2)]$ becomes high, we can get rid of ω_4 too. The main layout of our lowpass-bandpass section with its frequency response has been presented in Figure 3, where all dimensions are in mm and the width of all thin lines are 0.1 mm. As you can see in Figure 3, a disturbing harmonic is created between the two passbands, which must be removed after connecting to the BPF. The BPF should be designed and optimized to have a positive loading effect after connecting to the lowpass-bandpass cell. At the lower and upper channels, the ILs are two low values of 0.008 dB and 0.2 dB, respectively. Meanwhile, S_{11} is −27.7 dB at the lowpass and −16.6 dB at the bandpass channels. Above the upper channel, the harmonics have been suppressed up to 12 GHz. All microstrip structures in this work are simulated with an Advanced Design Systems using linear steps of an EM simulator. The substrate of all microstrip structure is a Rogers_RT_Duroid5880 with ε_r = 2.22, tan (δ) = 0.0009 and h = 0.7874 mm.

The spiral coupled lines with different widths have been used to design a bandpass resonator. This resonator and its approximate LC circuit are depicted in Figure 4. The capacitors (C) have been added to show the effect of coupling between lines. Half of the thin spiral line is replaced by the inductor L_T, and half of the thick spiral line is replaced by L_W.
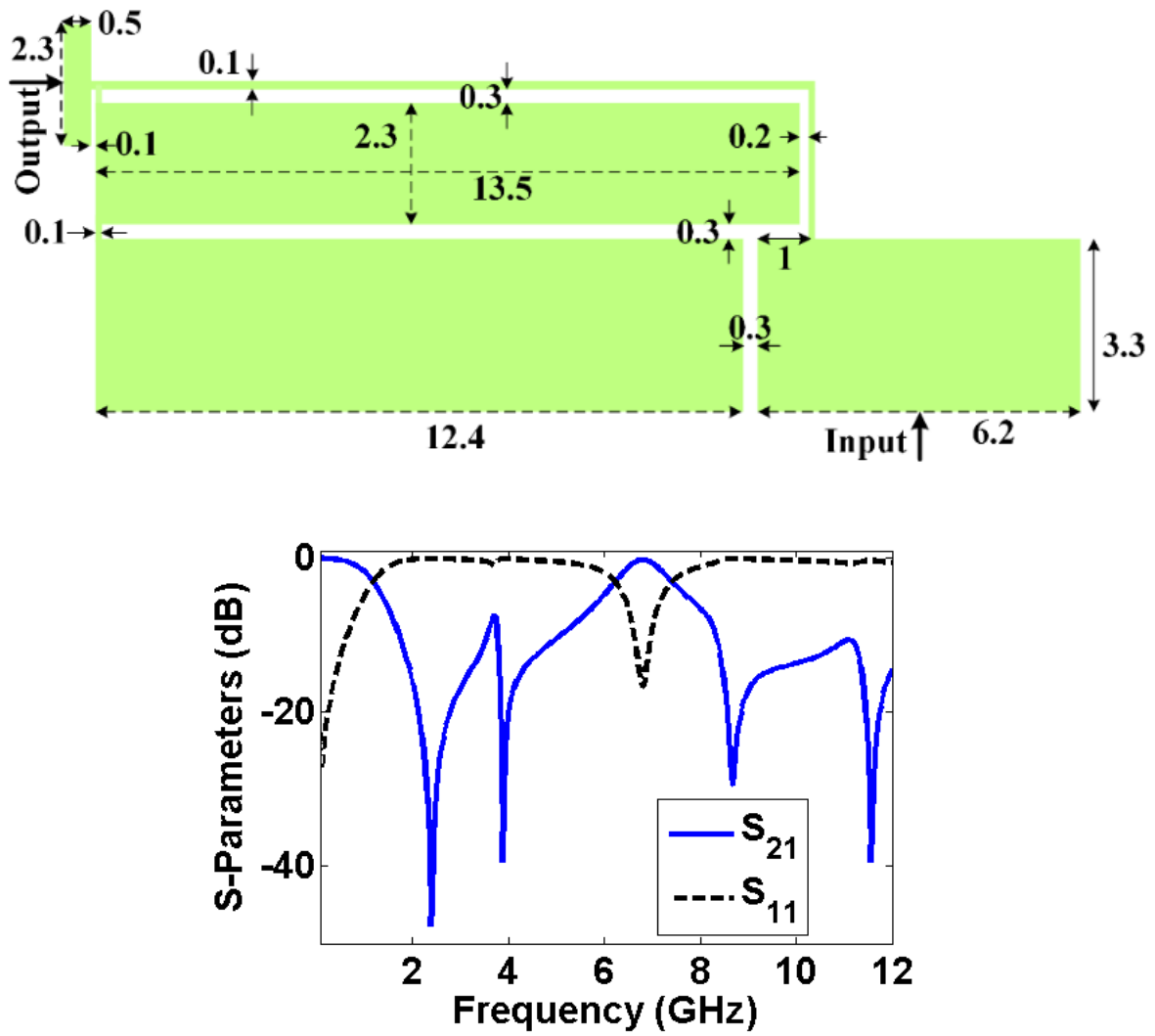
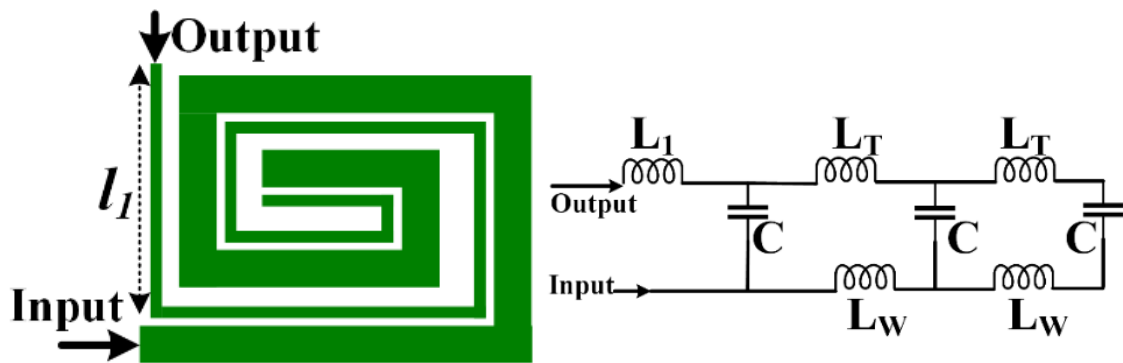**Figure 3.** Lowpass-bandpass structure with its frequency response.

Figure 4. Bandpass resonator and its approximate *LC* circuit.

To find out how this circuit works, we can first calculate the input impedance (Z_in) as follows:

$$Z_{in} = \frac{\left\{\frac{\left[\frac{1}{j\omega C}+j\omega(L_W+L_T)\right]\times\frac{1}{j\omega C}}{\frac{2}{j\omega C}+j\omega(L_W+L_T)}+j\omega(L_W+L_T)\right\}\times\frac{1}{j\omega C}}{\frac{\left[\frac{1}{j\omega C}+j\omega(L_W+L_T)\right]\times\frac{1}{j\omega C}}{\frac{2}{j\omega C}+j\omega(L_W+L_T)}+j\omega(L_W+L_T)+\frac{1}{j\omega C}}+j\omega L_1 \Rightarrow$$

$$Z_{in} = \frac{\frac{1}{j\omega C}+3j\omega(L_W+L_T)-j\omega^3 C(L_W+L_T)^2}{3-4\omega^2 C(L_W+L_T)+\omega^4 C^2(L_W+L_T)^2}+j\omega L_1 \Rightarrow$$

$$Z_{in} = \frac{1-3\omega^2 C(L_W+L_T+L_1)+\omega^4 C^2(L_W+L_T)[L_W+L_T+4L_1]-\omega^6 C^3 L_1(L_W+L_T)^2}{3j\omega C-4jC^2\omega^3(L_W+L_T)+j\omega^5 C^3(L_W+L_T)^2}$$

(6)

An angular resonance frequency (ω_a) can be calculated from Equation (6), as follows:

$$Z_{in}=\infty \Rightarrow 3-4C\omega_a^2(L_W+L_T)+\omega_a^3 C^2(L_W+L_T)^2=0$$
$$\omega_a^3 C^2(L_W+L_T)^2\langle\langle C\omega_a^2(L_W+L_T) \Rightarrow$$
$$\omega_a \approx \sqrt{\frac{3}{4C(L_W+L_T)}}$$

(7)

Another angular resonance frequency (ω_b) will be obtained as follows:

$$Z_{in}=0 \Rightarrow$$
$$1-3\omega_b^2 C(L_W+L_T+L_1)+\omega_b^4 C^2(L_W+L_T)[L_W+L_T+4L_1]-\omega_b^6 C^3 L_1(L_W+L_T)^2=0$$
$$\begin{cases}\omega_b^6 C^3 L_1(L_W+L_T)^2\rangle\rangle\omega_b^4 C^2(L_W+L_T)[L_W+L_T+4L_1]\\\omega_b^6 C^3 L_1(L_W+L_T)^2\rangle\rangle 3\omega_b^2 C(L_W+L_T+L_1)\end{cases} \Rightarrow \omega_b=\sqrt[6]{\frac{1}{C^3 L_1(L_W+L_T)^2}}$$

(8)

Since our goal is to design a BPF with a single resonant frequency, one of the angular resonant frequencies will be a harmonic. To solve this problem, the values of L_1, L_W and L_T can be adjusted so that $\omega_a = \omega_b$. This leads to:

$$\omega_a=\omega_b \Rightarrow \sqrt{\frac{3}{4C(L_W+L_T)}}=\sqrt[6]{\frac{1}{C^3 L_1(L_W+L_T)^2}} \Rightarrow \sqrt{\frac{3}{4}}=\sqrt[6]{\frac{L_W+L_T}{L_1}} \Rightarrow \frac{L_W+L_T}{L_1}\approx 0.42$$

(9)

It is enough to adjust the ratio of inductors based on (9) for eliminating a harmonic. Using this resonator, a BPF is designed and presented in Figure 5, where all dimensions are in mm; the width of each thin line is 0.1 mm and the space between coupled lines is 0.1 mm. This filter works at 3.67 GHz, which is suitable for WiMAX applications. It has a low insertion loss of 0.09 dB and a return loss (RL) of 17.4 dB. The harmonics have been attenuated up to 9.2 GHz with a maximum level of −20 dB.

By integrating BPF and lowpass-bandpass section, a three-channel diplexer is designed and presented in Figure 6. The overall size of proposed three-channel lowpass-bandpass diplexer is 19.5 mm × 7.6 mm, with a lowpass channel cut-off frequency of 1.22 GHz. Therefore, the size is only 0.103 λ_g × 0.04 λ_g = 0.004 $\lambda_g{}^2$, where λ_g is the guided wavelength calculated at 1.22 GHz. The fabricated diplexer is shown in Figure 6 too.

The current density distributions of the proposed diplexer for simulating ports 2 (at 1.22 GHz) and 3 (at 3.65 GHz) have been shown in Figure 6, respectively. The current density in a microstrip line depends on the width of the line. As the width of the transition line decreases, the current density increases. Hence, in Figure 7a,b, the thin lines have a higher current density. As shown for simulating each port, the resonator near it has a high current density. When we simulate port 3 at the resonance frequency of BPF, the thinner spiral cell has a high current density. Generally, the low impedance sections have less current density distributions.
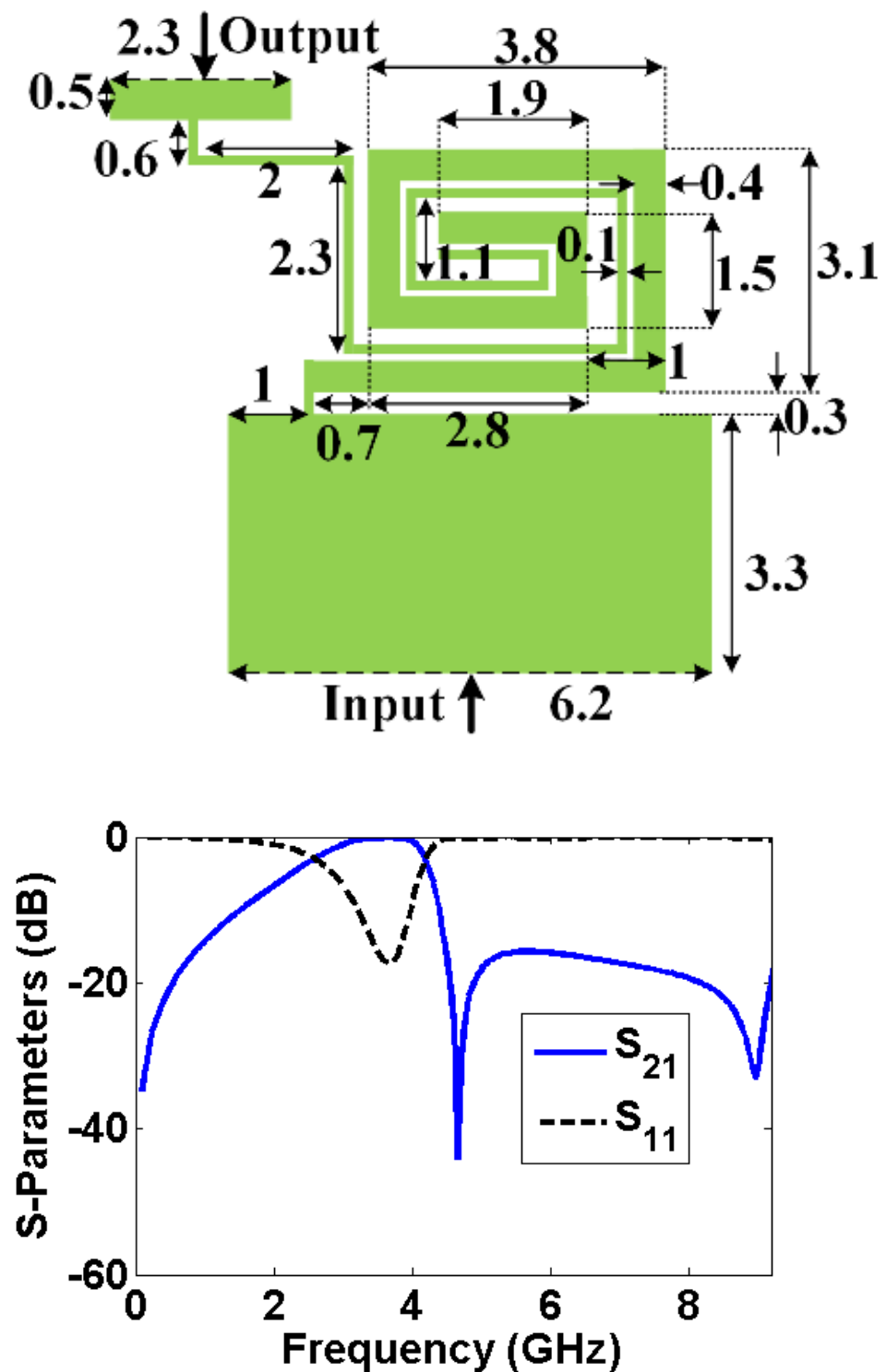
Figure 5. Layout of BPF and its frequency response.

Figure 8 illustrates the data flow diagram according to the proposed approach and the proposed structure shown in Figure 1. The first layer of the flow chart is all about the Metaverse and how it relates to the transportation system. Information collected in this layer includes data on vehicle locations, traffic flow, and routes, which are obtained from GPS systems, traffic cameras, and sensors embedded in roads and vehicles.
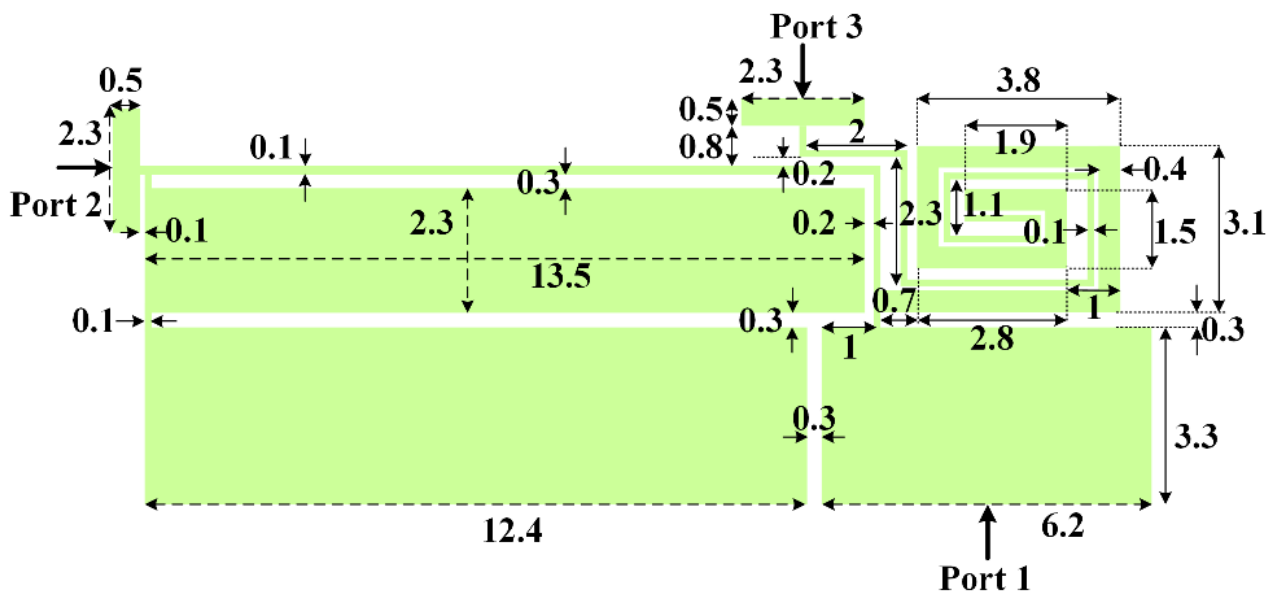
Figure 6. Three-channel diplexer with the dimensions in mm with a photograph of the fabricated diplexer.

The second layer of the flow chart is focused on a smart grid that uses 5G technology. The data collected in this layer pertain to energy consumption and distribution. Smart meters and other devices are used to gather information on energy usage, load balancing, and power grid stability. Layer 3 is specifically designed for IoT 5G devices, which include sensors, wearables, and smart home devices.
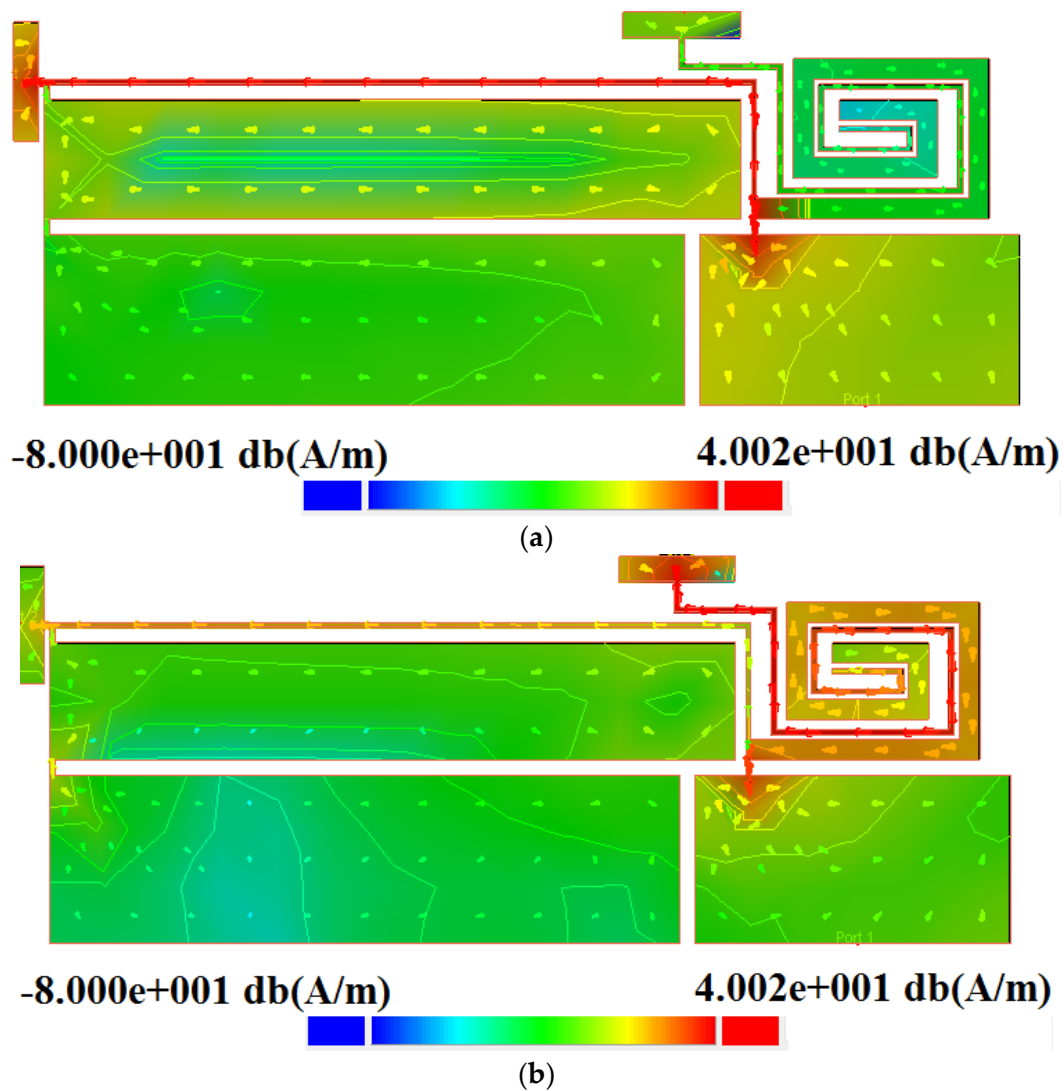
-8.000e+001 db(A/m)　　　　4.002e+001 db(A/m)

(**a**)

-8.000e+001 db(A/m)　　　　4.002e+001 db(A/m)

(**b**)

Figure 7. Current density distributions of the proposed diplexer for simulating (**a**) port 2 (at 1.22 GHz) and (**b**) port 3 (at 3.65 GHz).

The data collected from these devices encompasses usage patterns, environmental conditions, and other relevant metrics. Layer 4 is targeted towards different modes of transportation, such as cars, buses, and trains. The data gathered in this layer include information on routes, schedules, and capacity, which are used to improve transportation operations. Finally, Layer 5 is centered around a generator that provides power through sources such as electricity and gas. Data collected in this layer pertain to fuel consumption, emissions, and power output from power plants, substations, and smart grid devices, which are used to optimize energy production and distribution. Overall, these five layers work together to collect and analyze data related to transportation, energy, IoT devices, modes of transportation, and power generation. The insights gathered from this data are then used to optimize operations and improve efficiency, ultimately leading to a more interconnected and sustainable system
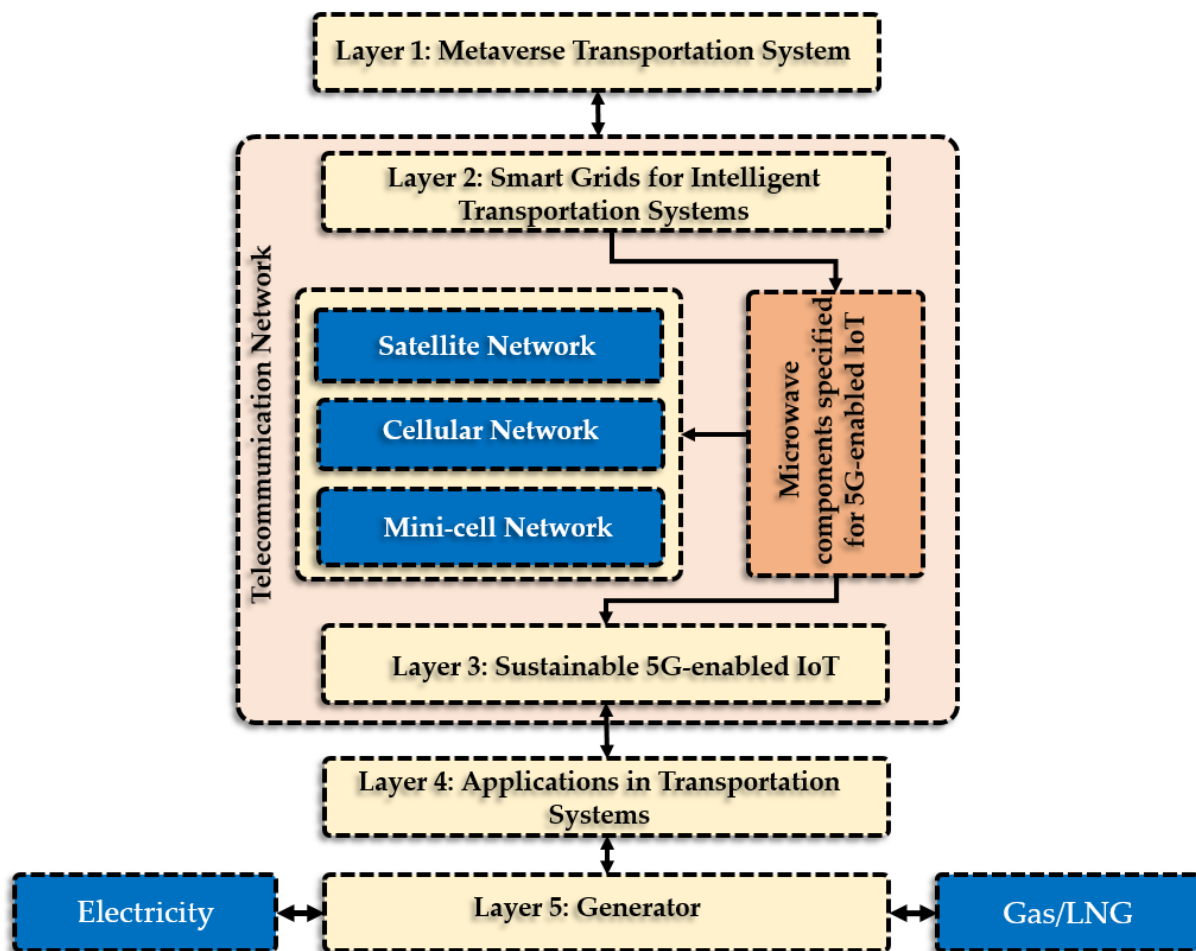
Figure 8. The Five Layers of Data Collection and Analysis: An Interconnected System for Sustainable Transportation and Energy. From the Metaverse to the transportation system, smart grid, IoT devices, modes of transportation, and power generation, data are being collected and analyzed to optimize operations and improve efficiency. With insights on energy consumption, environmental conditions, and transportation routes, this system aims to create a sustainable future through the integration of various layers of data collection and analysis.

4. Simulation and Measurement Results

The simulated and measured frequency response of the proposed diplexer is depicted in Figure 9. The measurement results verify simulations where they are obtained using a HP8757A network analyser. The resonance frequencies of middle and upper channels are 3.65 GHz and 6.79 GHz, respectively. Moreover, the FBW of the middle and last channels are 53.2% and 17.6%, respectively. The ILs at the lower, middle, and higher channels are 0.006 dB, 0.11 dB and 0.16 dB, respectively, while these channels have three RLs of 29.6 dB, 17.6 dB, and 19.7 dB, respectively. Due to copper and SMA losses, the simulation results are a little better than measurements. The harmonics have been suppressed up to 9 GHz, with a maximum level of −18 dB. Therefore, our diplexer can suppress the harmonics up to the 6th harmonic. The isolation between ports 2 and 3 is better than −20 dB from DC to 7.6 GHz.
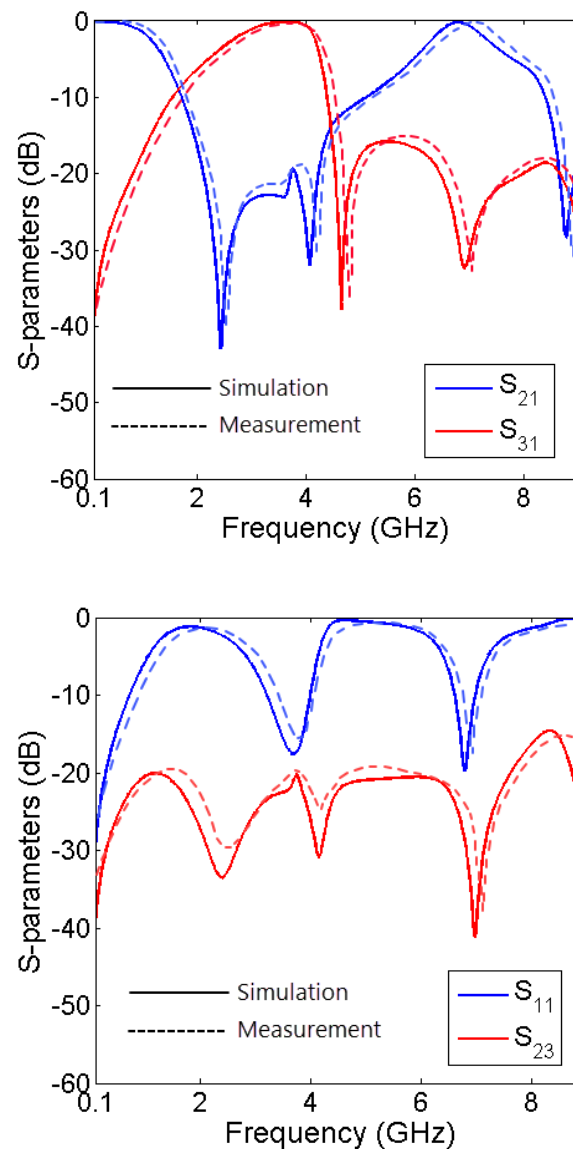
Figure 9. Simulated and measured S-Parameters of our three-band diplexer.

In order to show the advantage of our device, we compared it with previous works in Table 1. As shown in Table 1, our diplexer is the most compact with the lowest insertion losses. Moreover, our lowpass channel is the widest channel with a maximum fractional bandwidth in comparison with previous works. Furthermore, the best value of RL at the lowpass channel is obtained in this work.

The group delays at the lower, middle, and higher passbands are presented in Figure 10. The maximum group delays at the lower, middle, and higher passbands are 0.33 ns, 1.7 ns, and 0.34 ns, respectively. In order to show the flatness of all passbands, the group delay of this diplexer is compared with previous works, and the results have been presented in Table 2. As depicted in Table 2, minimum group delay is achieved in this work, which verifies the flatness of channels.

Table 1. Comparison between our diplexer and previous works (NC: Number of Channels, *: Approximated values).

| Refs	ILs (dB)	RLs (dB)	−3 dB FBWs	Size (λg²)	NC	Type
Our Diplexer	0.006, 0.1, 0.1	29.6, 17.6, 19.7	53.2%, 17.6%	0.004	3	Lowpass-Bandpass Diplexer
[8]	0.25, 2.42	—	7.6%	—	2	Lowpass-Bandpass Diplexer
[9]	0.12, 0.1	19, 36	23.8%	0.03	2	Lowpass-Bandpass Diplexer
[11]	0.4, 0.33, 0.35, 0.45	19, 19, 19, 20	0.2, 0.2, 0.2, 0.2	1.1	4	Bandpass Diplexer
[12]	0.75, 0.89, 2.8	—	17.6%, 11.8%, 7.7%	0.09	3	BPF
[13]	2.7, 2.5, 1.8	16, 16, 16	6.5%, 7.3%, 8.2%	0.048	3	Bandpass Triplexer
[14]	0.8, 2.1, 2.5	14.5, 12, 12.9	10%, 7%	0.067 *	3	Lowpass-Bandpass Triplexer
[16]	1.35, 1.31	15, 15	8.2%, 7.69%	0.05	2	Bandpass Diplexer
[17]	0.09, 0.5	21.5, 22.4	8.7%, 6%	0.193	2	Bandpass Diplexer
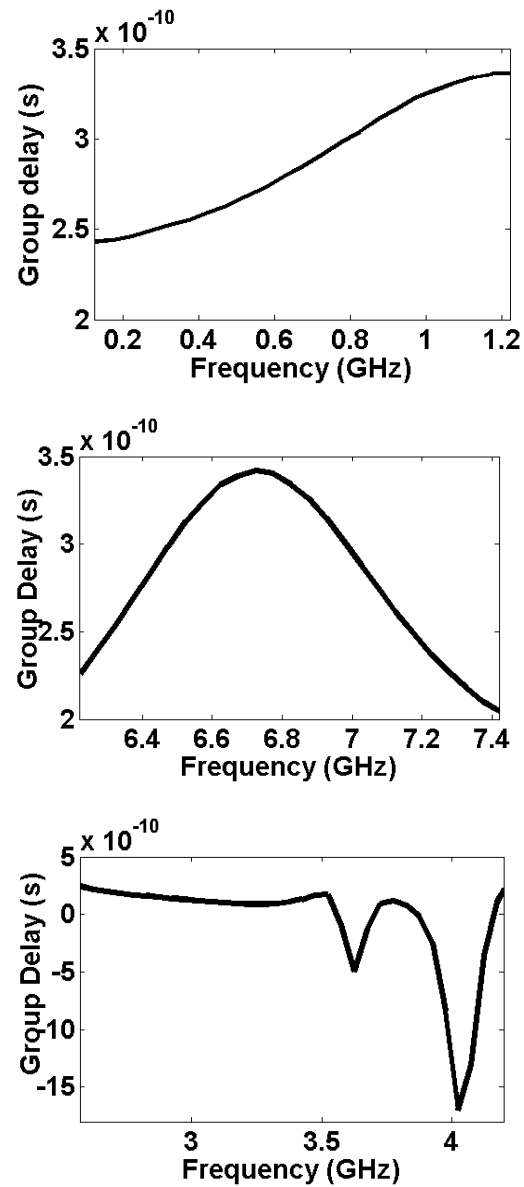
Figure 10. Group delay at the lower, middle, and higher passbands.

Table 2. Group delay of this diplexer in comparison with the previous works.

Refs	Group Delays (ns)	Type
This diplexer	0.34, 1.7, 0.34	Three-Channel Lowpass-Bandpass Diplexer
[[**9**]]	2, 1.24	Dual-Channel Lowpass-Bandpass Diplexer
[**14**]	1.5, 6, 4.4	Lowpass-Bandpass Triplexer
[**24**]	Maximum 8	Three-Band BPF
[**25**]	3.67, 1.47, 0.83	Three-Band BPF
[**26**]	9, 6, 6, 5	Quad-Band Filter

5. Discussion

Presently, the Metaverse is a popular subject of research in various fields and is currently experiencing the most rapid growth in the high-tech industry [27,28]. The importance of data processing and interpretation is also increasing, especially for engineers, due to the digitization of energy systems. Smart grids include a range of new data-driven services, such as usage monitoring, energy storage, marketing, and the supply of renewable energy [21]. On the other hand, some intelligent solutions such as prediction can be useful. For example, traffic prediction as a crucial infrastructure for a wide range of applications in transportation systems, such as route planning and vehicular communications, has been investigated. However, accurately predicting traffic patterns is difficult because traffic networks have dynamic and diverse spatial–temporal correlations [29]. In another research, a reliable and secure communication in a wireless-powered non-orthogonal multiple access (NOMA) system in the presence of multiple eavesdroppers has been investigated. To ensure the system's reliability and security, the authors proposed a joint artificial noise and power allocation (JAP) scheme [30].

The popularity and manufacturing of electric vehicles (EVs) are increasing due to their positive impact on the environment [31]. This paper introduces an effective diplexer for 5G-enabled IoT in smart grids and the Metaverse, which is based on the latest advancements and fundamentals in modern energy distribution. The integration of 5G-enabled IoT in energy distribution can significantly enhance the speed and efficiency of data handling, including tasks such as big data analytics, managing energy devices and materials, optimizing transmission and distribution infrastructure, providing energy to individual consumers, and transmitting energy from transmission systems. In this study, we examined the various challenges faced by smart grids and the Metaverse, analyze recent developments in transportation, and evaluate the impact of 5G-enabled IoT on the energy industry. We also propose a conceptual framework that can be used to address complex issues.

The mobility of vehicles and pedestrians can make transportation data prone to inaccuracies, incompleteness, or unreliability, particularly in specific locations or at certain times. For instance, not all vehicles have the technology required to provide real-time location data, and road traffic data from sensors on the road can be missing. One way to overcome these challenges is by investing in new data collection technologies to improve data collection capabilities [1].

The implementation of self-driving technology will greatly improve Intelligent Transportation Systems. AUVs can utilize existing road networks more efficiently than human-driven cars by traveling in compact groups or convoys. Additionally, AUVs can make use of dedicated lanes, such as those that require payment, by maintaining a "train on wheel" formation and switching lanes in a safer and more efficient manner than human drivers. AUVs can also handle automatic payment processing and participate in auctions or bids on the behalf of customers. If necessary, they can report non-compliant vehicles to enforce payment. In terms of safety, AUVs can detect and track other road users, such as pedestrians and cyclists, using sophisticated sensors and Lidars. They can then communicate this information to other vehicles via V2V communication, such as warning of a "bike ahead" and suggesting lane changes [2].

Sustainability is crucial for successful interactions, whether in real-life relationships or in the Metaverse. To maintain continuous interactions in the Metaverse, users must recognize the benefits and convenience of staying for extended periods. If the number of visits and users decreases, it can hinder growth [5]. Additionally, users must have access to high-speed internet to participate in the Metaverse. Unfortunately, a significant portion of the world lacks such fast internet access, which raises concerns about the sustainability of the Metaverse. What happens if half the world suddenly loses access to the Metaverse? This could be disastrous, particularly if a remote driver is navigating a vehicle in the Metaverse or real world and loses internet connection, leading to potential fatalities. Therefore, it is essential to consider the sustainability of the Metaverse in terms of internet access and potential real-world consequences [5,14]. Intelligent vehicles in the MTS use different types of sensors such as millimeter-wave radar, lidar, cameras, and satellite navigation to detect the surrounding environment. They gather information and analyze static and dynamic objects using prediction methods. By utilizing navigation map data, intelligent vehicles perform systematic calculations [3].

Generated virtual data have several advantages over real data, including the ease of collection and comprehensive annotation of information. Virtual data are expandable in scale and diversity since it is possible to obtain diverse data by setting different physical models and parameters. The virtual space can restore various scenes with fixed parameters, which allow evaluation of vision models from different angles. Additionally, virtual data can be generated in situations where visual data cannot be obtained in real scenes, such as high-speed rail line fault detection and battlefield data detection, making it feasible to design and validate vision models [3].

To sum up, the use of microstrip components such as the suggested diplexer offers numerous benefits for sustainable IoT in smart grids and the Metaverse. The primary advantage of microstrip technology is its cost-effectiveness, as it requires only a two-layer board with all components mounted on a single side [32,33]. This eliminates the need for ways when making connections, thereby avoiding unwanted capacitance or inductance. Microstrip traces provide better control over the characteristic impedance of the trace, ensuring that the circuit operates within the intended frequency range. Furthermore, microstrip traces have wider widths, making them less sensitive to changes in width due to over-etching during fabrication, which is essential in RF circuit board design. Overall, microstrip components are a cost-effective, efficient, and precise solution for building sustainable IoT networks in smart grids and the Metaverse, especially in high-frequency applications such as 5G networks.

6. Conclusions

In conclusion, this study proposes the integration of transportation technology with the Metaverse through the Metaverse Transportation System (MTS) to enhance the efficiency and intelligence of real-world transportation systems. To ensure sustainability, the design of MTS prioritizes energy conservation and efficiency, incorporating 5G-enabled IoT and sensor networks. This study focuses on developing a highly efficient three-channel microstrip lowpass-bandpass diplexer, which is a crucial component for implementing 5G-enabled IoT in MTS. The proposed diplexer is compared with previous works, and the results demonstrate its small size, flat channels, and low losses. The cut-off and resonance frequencies of the diplexer are at 1.22 GHz, 3.65 GHz, and 6.79 GHz, making it suitable for wireless applications, including 5G. This study's findings show that the proposed diplexer outperforms previous multi-channel diplexers in terms of size and performance. In future work, this study's findings can be used to design and implement more efficient and sustainable transportation systems through MTS.

References

1. Zhu, L.; Yu, F.R.; Wang, Y.; Ning, B.; Tang, T. Big data analytics in intelligent transportation systems: A survey. *IEEE Trans. Intell. Transp. Syst.* **2018**, *20*, 383–398. [CrossRef]
2. Gerla, M.; Lee, E.-K.; Pau, G.; Lee, U. Internet of vehicles: From intelligent grid to autonomous cars and vehicular clouds. In Proceedings of the 2014 IEEE world forum on internet of things (WF-IoT), Seoul, Republic of Korea, 6–8 March 2014; pp. 241–246.
3. Zhang, H.; Luo, G.; Li, Y.; Wang, F.-Y. Parallel Vision for Intelligent Transportation Systems in Metaverse: Challenges, Solutions, and Potential Applications. *IEEE Trans. Syst. Man Cybern. Syst.* **2022**. [CrossRef]
4. Jamshidi, M.B.; Ebadpour, M.; Moghani, M.M. Cancer Digital Twins in Metaverse. In Proceedings of the 2022 20th International Conference on Mechatronics-Mechatronika (ME), Pilsen, Czech Republic, 7–9 December 2022; pp. 1–6.
5. Njoku, J.N.; Nwakanma, C.I.; Amaizu, G.C.; Kim, D.S. Prospects and challenges of Metaverse application in data-driven intelligent transportation systems. *IET Intell. Transp. Syst.* **2023**, *17*, 1–21. [CrossRef]
6. Wu, H.-W.; Huang, S.-H.; Chen, Y.-F. Design of new quad-channel diplexer with compact circuit size. *IEEE Microw. Wirel. Compon. Lett.* **2013**, *23*, 240–242. [CrossRef]
7. Jamshidi, M.B.; Roshani, S.; Talla, J.; Roshani, S.; Peroutka, Z. Size reduction and performance improvement of a microstrip Wilkinson power divider using a hybrid design technique. *Sci. Rep.* **2021**, *11*, 7773. [CrossRef]
8. Deng, P.-H.; Tsai, J.-T. Design of microstrip lowpass-bandpass diplexer. *IEEE Microw. Wirel. Compon. Lett.* **2013**, *23*, 332–334. [CrossRef]
9. Hayati, M.; Rezaei, A.; Noori, L. Design of a high–performance lowpass–bandpass diplexer using a novel microstrip structure for GSM and WiMAX applications. *IET Circuits Devices Syst.* **2019**, *13*, 361–367. [CrossRef]
10. Yahya, S.I.; Nouri, L. A low-loss four-channel microstrip diplexer for wideband multi-service wireless applications. *AEU-Int. J. Electron. Commun.* **2021**, *133*, 153670. [CrossRef]
11. Heng, Y.; Guo, X.; Cao, B.; Wei, B.; Zhang, X.; Zhang, G.; Song, X. A narrowband superconducting quadruplexer with high isolation. *IEEE Trans. Appl. Supercond.* **2014**, *24*, 21–26. [CrossRef]
12. Zheng, S.Y.; Su, Z.L.; Pan, Y.M.; Qamar, Z.; Ho, D. New dual-/tri-band bandpass filters and diplexer with large frequency ratio. *IEEE Trans. Microw. Theory Tech.* **2018**, *66*, 2978–2992. [CrossRef]
13. Wu, J.-Y.; Hsu, K.-W.; Tseng, Y.-H.; Tu, W.-H. High-isolation microstrip triplexer using multiple-mode resonators. *IEEE Microw. Wirel. Compon. Lett.* **2012**, *22*, 173–175. [CrossRef]
14. Chen, F.-C.; Qiu, J.-M.; Hu, H.-T.; Chu, Q.-X.; Lancaster, M.J. Design of microstrip lowpass-bandpass triplexer with high isolation. *IEEE Microw. Wirel. Compon. Lett.* **2015**, *25*, 805–807. [CrossRef]
15. Rezaei, A.; Noori, L. Novel low-loss microstrip triplexer using coupled lines and step impedance cells for 4G and WiMAX applications. *Turk. J. Electr. Eng. Comput. Sci.* **2018**, *26*, 1871–1880. [CrossRef]
16. Bukuru, D.; Song, K. Compact wide-stopband planar diplexer based on rectangular dual spiral resonator. *Microw. Opt. Technol. Lett.* **2015**, *57*, 174–178. [CrossRef]
17. Chinig, A.; Zbitou, J.; Errkik, A.; Tajmouati, A.; El Abdellaoui, L.; Latrach, M.; Tribak, A. Microstrip diplexer using stepped impedance resonators. *Wirel. Pers. Commun.* **2015**, *84*, 2537–2548. [CrossRef]
18. Jamshidi, M.; Roshani, S.; Roshani, S.; Talla, J. A compact low-pass filter with simple structure and sharp roll-off. In Proceedings of the 2020 International Conference on Applied Electronics (AE), Pilsen, Czech Republic, 8–9 September 2020; pp. 1–4.
19. Jamshidi, M.B.; Daneshfar, F. A Hybrid Echo State Network for Hypercomplex Pattern Recognition, Classification, and Big Data Analysis. In Proceedings of the 2022 12th International Conference on Computer and Knowledge Engineering (ICCKE), Mashhad, Iran, 17–18 November 2022; pp. 007–012.
20. Carrillo, D.; Kalalas, C.; Raussi, P.; Michalopoulos, D.S.; Rodríguez, D.Z.; Kokkoniemi-Tarkkanen, H.; Ahola, K.; Nardelli, P.H.; Fraidenraich, G.; Popovski, P. Boosting 5G on smart grid communication: A smart RAN slicing approach. *IEEE Wirel. Commun.* **2022**. [CrossRef]
21. Shafiei, A.; Jamshidi, M.; Khani, F.; Talla, J.; Peroutka, Z.; Gantassi, R.; Baz, M.; Cheikhrouhou, O.; Hamam, H. A Hybrid Technique Based on a Genetic Algorithm for Fuzzy Multiobjective Problems in 5G, Internet of Things, and Mobile Edge Computing. *Math. Probl. Eng.* **2021**, *2021*, 1–14. [CrossRef]
22. Daneshfar, F.; Jamshidi, M.B. A Pattern Recognition Framework for Signal Processing in Metaverse. In Proceedings of the 2022 8th Iranian Conference on Signal Processing and Intelligent Systems (ICSPIS), Mazandaran, Iran, 28–29 December 2022; pp. 1–5.

23. Hong, J.-S.G.; Lancaster, M.J. *Microstrip Filters for RF/Microwave Applications*; John Wiley & Sons: Hoboken, NJ, USA, 2004.
24. Liu, Y.; Dou, W.-B.; Zhao, Y.-J. A tri-band bandpass filter realized using tri-mode T-shape branches. *Prog. Electromagn. Res.* **2010**, *105*, 425–444. [CrossRef]
25. Wibisono, G.; Firmansyah, T.; Syafraditya, T. Design of Triple-Band Bandpass Filter Using Cascade Tri-Section Stepped Impedance Resonators. *J. ICT Res. Appl.* **2016**, *10*. [CrossRef]
26. Lin, S.-C. Microstrip dual/quad-band filters with coupled lines and quasi-lumped impedance inverters based on parallel-path transmission. *IEEE Trans. Microw. Theory Tech.* **2011**, *59*, 1937–1946. [CrossRef]
27. Khalaj, O.; Jamshidi, M.; Hassas, P.; Hosseininezhad, M.; Mašek, B.; Štadler, C.; Svoboda, J. Metaverse and AI Digital Twinning of 42SiCr Steel Alloys. *Mathematics* **2022**, *11*, 4. [CrossRef]
28. Ebadpour, M.; Jamshidi, M.; Talla, J.; Hashemi-Dezaki, H.; Peroutka, Z. Digital Twin Model of Electric Drives Empowered by EKF. *Sensors* **2023**, *23*, 2006. [CrossRef] [PubMed]
29. Long, W.; Xiao, Z.; Wang, D.; Jiang, H.; Chen, J.; Li, Y.; Alazab, M. Unified Spatial-Temporal Neighbor Attention Network for Dynamic Traffic Prediction. *IEEE Trans. Veh. Technol.* **2022**. [CrossRef]
30. Cao, K.; Wang, B.; Ding, H.; Lv, L.; Tian, J.; Hu, H.; Gong, F. Achieving reliable and secure communications in wireless-powered NOMA systems. *IEEE Trans. Veh. Technol.* **2021**, *70*, 1978–1983. [CrossRef]
31. Xiao, Y.; Zhang, Y.; Kaku, I.; Kang, R.; Pan, X. Electric vehicle routing problem: A systematic review and a new comprehensive model with nonlinear energy recharging and consumption. *Renew. Sustain. Energy Rev.* **2021**, *151*, 111567. [CrossRef]
32. Roshani, S.; Koziel, S.; Roshani, S.; Jamshidi, M.B.; Parandin, F.; Szczepanski, S. Design of a patch power divider with simple structure and ultra-broadband harmonics suppression. *IEEE Access* **2021**, *9*, 165734–165744. [CrossRef]
33. Jamshidi, M.B.; Roshani, S.; Talla, J.; Sharifi-Atashgah, M.S.; Roshani, S.; Peroutka, Z. Cloud-based machine learning techniques implemented by microsoft azure for designing power amplifiers. In Proceedings of the 2021 IEEE 12th Annual Ubiquitous Computing, Electronics & Mobile Communication Conference (UEMCON), New York, NY, USA, 1–4 December 2021; pp. 0041–0044.